Railway Engineering Science
https://doi.org/10.1007/s40534-026-00433-8

Integration of fatigue life assessment into structural optimization of a railway vehicle bogie frame: development and application of a new methodology

Alessio Cascino[1] · **Lorenzo Giannelli**[1] · **Enrico Meli**[1] · **Andrea Rindi**[1]

Received: 6 June 2025 / Revised: 3 February 2026 / Accepted: 3 February 2026

Abstract
Rolling stock manufacturers are increasingly developing innovative structural solutions aimed at enhancing the quality and reliability of railway vehicle components, thereby enhancing the existing standard platforms. Structural optimization processes represent an effective strategy to reduce manufacturing costs by promoting geometries that are simpler to design and fabricate. While structural optimization is now a well-established practice in the railway sector, the integration of fatigue considerations into this process remains limited. Although several studies in the literature attempt to address fatigue through various approaches, none have proven entirely satisfactory. This research aims to bridge this gap by introducing a novel methodology capable of automatically computing fatigue-related parameters, thereby enabling a parallel fatigue performance evaluation throughout the entire optimization process, iteration by iteration. The methodology is implemented via a dedicated software tool, which can be adapted with minimal modifications to interface with most commercial finite element platforms. The proposed approach has been applied to the structural optimization of a metro bogie frame. The methodology was then employed in multiple activities: iterative fatigue monitoring during the optimization process; extension of a previous study by incorporating fatigue behavior; reconstruction of the final post-optimization geometry based on fatigue-driven design considerations, thus ensuring manufacturability and fatigue resistance. Although not all potential uses have been fully explored, the proposed methodology has demonstrated its effectiveness as a valuable tool for integrating fatigue into structural optimization, ultimately enabling the designer to reconstruct fatigue-aware final geometries.

Keywords Structural topological optimization · Fatigue assessment · Railway vehicle dynamics · Railway engineering · Railway vehicle design · Casting design

1 Introduction

Rail transport, including trains, trams, and metro systems, plays a crucial role in the development of sustainable and efficient urban and interurban mobility. As global demand for reliable, high-capacity public transportation continues to rise, rail systems are increasingly being expanded and modernized. In this context, the reliability of rail vehicles has become a key factor in ensuring consistent and high-quality service. Achieving this goal requires a holistic and integrated design approach that considers all aspects of vehicle performance, safety, and durability. Among these, mechanical fatigue represents a critical challenge: despite advances in materials and simulation tools, fatigue-related issues remain one of the least controllable parameters in the design process. This limitation has often led to unexpected failures and increased maintenance efforts. Addressing mechanical fatigue more effectively through integrated and predictive design methodologies is therefore essential to enhancing the long-term reliability and efficiency of rail transport systems.

Structural optimization plays a pivotal role in the pursuit of more reliable and efficient rail vehicles. By systematically improving the design of components and assemblies, structural optimization enables engineers to minimize weight while maintaining or enhancing strength, stiffness, and fatigue resistance. This is particularly important in rail applications, where reducing mass can lead to lower energy

✉ Alessio Cascino
alessio.cascino@unifi.it

[1] Department of Industrial Engineering, University of Florence, Florence, Italy

consumption, reduced track wear, and improved dynamic performance. Moreover, optimization techniques, such as topology, shape, and size optimization, allow for the identification of innovative design solutions that may not be evident through traditional engineering approaches. When integrated early in the design process, structural optimization not only contributes to better mechanical performance but also helps in addressing critical reliability concerns, such as fatigue behavior, by distributing stresses more evenly and eliminating critical hotspots. As such, it represents a powerful tool for developing next-generation rail vehicles that meet the increasing demands for performance, safety, and sustainability.

In general, topological and structural optimization methods serve as powerful tools for designing a wide range of component types across various applications. Several recent applications have demonstrated the use of structural optimization in the field of robotics. A simulation-based reliability design optimization method is proposed to improve the reliability of robot structural design [1]. A hybrid multibody system (MBS) simulation—that is, an MBS containing flexible bodies—in conjunction with a co-simulation of the control system represented by tools of the Computer Aided Control Engineering (CACE) is integrated into the optimization process of a humanoid robotic system [2]. Other applications related to robotics have been applied to a general manipulator and a rehabilitation system [3, 4]. The design procedure of various turbomachinery components has been improved by adopting structural optimization approaches, especially if combined with additive manufacturing techniques [5–8].

Structural optimization techniques have been extensively applied in the automotive sector to improve vehicle performance while reducing weight and material usage. In particular, recent studies have explored multi-objective optimization approaches and advanced methodologies aimed at designing more efficient car body structures, balancing conflicting requirements such as stiffness, crashworthiness, and manufacturability [9, 10]. These works highlight the effectiveness of optimization strategies in addressing complex engineering challenges in modern vehicle design. Building on these approaches, more recent studies have also looked at how structures behave under large deformations, especially in safety-related parts of vehicles. Nonlinear optimization methods have been used to better model and improve the performance of these components during crash events [11].

In the railway sector, a structural optimization methodology was developed to achieve a lightweight carbody design while ensuring fatigue resistance through a multidisciplinary design optimization framework that integrates structural, material, and fatigue constraints [12]. A similar approach focusing on material selection combined with size optimization was applied to an EMU carbody, effectively reducing weight while maintaining mechanical performance and manufacturing feasibility [13]. A comparative study on aluminum and carbon fiber thin-walled structures for railway car bodies was conducted, focusing on dynamic behavior and size optimization to reduce weight while ensuring structural integrity [14]. Furthermore, a holistic strategy for lightweight design was proposed through an integrated optimization perspective that considers structural efficiency from the early stages of railway vehicle development [15].

The integration of dynamic performance considerations into structural optimization processes has proven essential for the development of lightweight railway carbodies that meet both mechanical and operational demands. A dynamic size optimization approach has been proposed to support the lightweight design process by incorporating modal and frequency response constraints, ensuring that the reduced-weight structure maintains adequate dynamic behavior under service conditions [16]. In a complementary study, a comprehensive strategy was introduced that combines the use of composite materials with dynamic structural optimization, highlighting how coupling material innovation with dynamic analysis can lead to more efficient and robust carbody designs [17].

Shifting perspective, even complex components such as the bogie frame and the bolster beam have shown attempts at innovation through the use of structural optimization processes. The application of topology optimization techniques to reduce the weight of an Indian railway freight bogie side frame has been explored [18], trying to reduce the mass of the system. Similarly, a methodology was developed for the design enhancement of railway bolster beams by applying topological optimization while accounting for manufacturing constraints. This approach allowed for a significant reduction in mass without compromising structural performance, supporting more efficient and feasible component designs [19]. A topology optimization was performed using the SIMP method with the goal of enhancing the structural stiffness. In parallel, the bogie frame of a tilting train operating in the Korean railway system was reengineered using an optimization technique based on a microgenetic algorithm [20]. The behavior of bogie frames under actual service loads has been simulated by integrating multibody dynamics with finite element analysis [21]. In a different study, a comprehensive design procedure was developed that combines topological optimization, CAD modeling, and multibody simulation, specifically applied to the development of a tram motor bogie frame. This approach, based on European standards [22], integrates finite element and dynamic analysis with technological constraints suited for casting production. The resulting design demonstrated improved structural efficiency and maintained dynamic performance, confirming the effectiveness of this integrated method [23].

Furthermore, the literature highlights the critical role of predicting the service life of railway bogie frames. Recent contributions in the literature have emphasized the importance of accounting for both uncertainty and experimental validation in the fatigue assessment of heavy vehicle frames. On one hand, lifetime assessment and structural optimization of welded frames under uncertain material properties, geometrical deviations, and loading conditions have proven effective in improving the reliability of complex structural components [24]. On the other hand, experimental fatigue evaluations conducted on metro train bogie frames have provided essential data for validating numerical models and understanding real-world fatigue behavior under service conditions [25]. In another study [26], the fatigue life assessment of high-speed railway bogie frames was performed by considering the effects of gear meshing, which introduce additional dynamic loads. This approach enables more accurate predictions of fatigue behavior and improves the reliability of bogie frame designs under complex operating conditions. Additionally, the lifetime assessment and structural optimization of a welded A-type frame in a mining truck has been carried out by Li et al., taking into account uncertainties related to material properties, geometry, and loading conditions. Their work demonstrated the benefits of incorporating probabilistic approaches to enhance design reliability and performance [24].

Building upon the established framework, this study aims to integrate fatigue life assessment of complex railway components, such as bogies, with structural optimization processes. In the railway sector, stress states are almost always multiaxial in nature, even when they are highly localized, which requires the identification of the most critical loading condition. For this reason, a dedicated optimization code was developed within this work to identify the maximum local stress state acting on the bogie frame, as resulting from all tested load cases. This approach enabled continuous monitoring of the system fatigue performance throughout the structural optimization process applied through finite element modeling, introducing a significant innovation in the bogie design phase. The optimization process also includes manufacturing constraints specifically oriented toward castability, facilitating the realization of the component through casting.

2 Materials and Methodology

This section outlines the methodology adopted throughout the current research activity. The railway bogie frame is described in detail, including the characteristics of the finite element (FE) model. Subsequently, the structural optimization process, a comprehensive analysis of the fatigue assessment methods applied in railway field and a detailed description of the adopted mathematical formalism are presented.

2.1 Model description: the bogie frame

The metro bogie frame serves as a fundamental structural element, engineered to support and integrate multiple components within the train underbody structure. Designed to withstand the rigorous demands of metro operations, the frame offers essential strength, reliability, and resistance to the intense dynamic loads acting due to track irregularities. It is fabricated using advanced precision and automated welding methods, which ensure uniformity and structural continuity across the steel assemblies. Nevertheless, these welded joints constitute a primary point of concern for railway bogie frames, particularly regarding mechanical fatigue under cyclic loading. The frame architecture comprises a combination of longitudinal beams, cross-members, and other geometrical features arranged to optimize load distribution throughout the structure in each possible condition. This configuration not only enhances the stability of the bogie but also plays a significant role in maintaining the safety and performance of the metro vehicle. The end crossbeams are essential for the resistance to torsional loads. In addition, emphasis was placed on the hollow section located beneath the secondary suspension housing, which is specifically designed to allow the traction link to pass through and connect appropriately to the bolster beam at the opposite end. The original bogie frame was manufactured from structural steel and fully assembled by welding, as depicted in Fig. 1. All the main interfaces with secondary systems and all supports have been highlighted in black. The global metal body of the bogie frame has been reported in gray.

2.2 Model description: FE model characteristics

The FE model of the initial bogie frame served as a high-fidelity representation of the system, developed using commercial software. Figure 2 presents an overview of the model

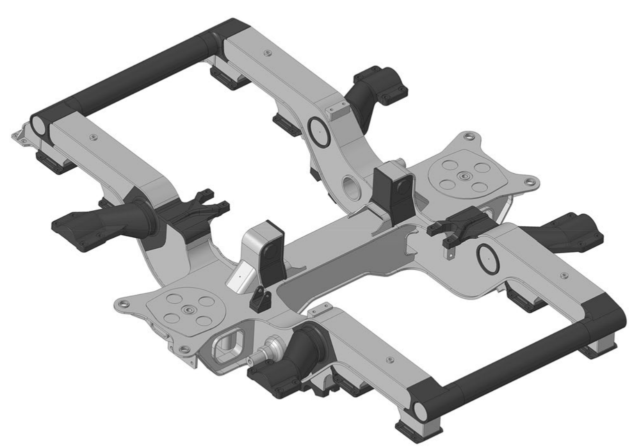

Fig. 1 Original metro bogie frame

 Springer

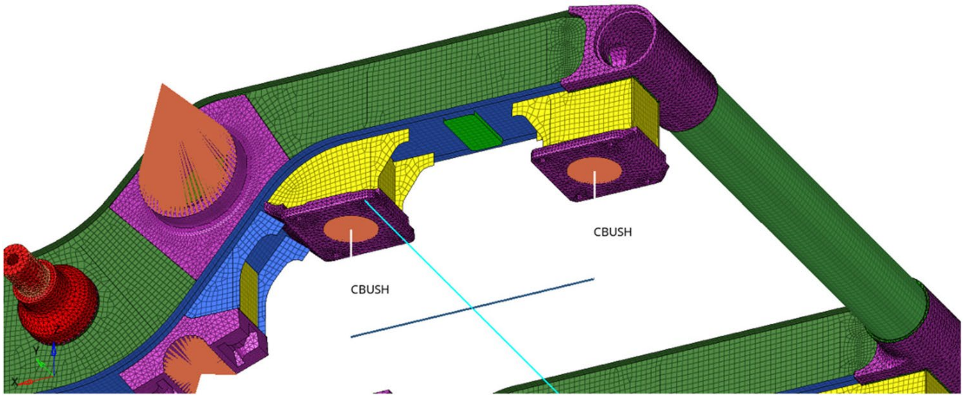

Fig. 2 FE model detailed view of the original metro bogie frame

along with a detailed view of the mesh in one of the most critical regions, as well as a close-up of the primary suspension linked to the axle. The primary components, comprising the central crossbeam, longitudinal beams, and end crossbeams, were discretized using a two-dimensional mesh made of QUAD4-type SHELL elements, with an average element size of 10 mm and a minimum of 3 mm. A mesh sensitivity analysis was carried out to validate the mesh quality, ensuring accurate stress predictions and overall reliability of the simulation. In contrast, all the support components described previously were modeled with a three-dimensional mesh using second-order TETRA elements (TETRA10), adopting the same size parameters as the shell elements. The selection of element types was guided by the geometric and structural characteristics of the components: the relatively thin sections of the bogie frame were well represented by shell elements, whereas the volumetric nature of the supports necessitated the use of solid elements. Since direct coupling between first-order 2D elements and 3D solid elements is not feasible, an effective interface strategy was employed. A freeze/bonded contact configuration was used to integrate the solid-meshed supports with the shell-meshed frame. This approach preserves model linearity and ensures complete stress transfer, including both forces and moments, by enforcing zero relative motion at the interface, maintaining a fixed gap and preventing any sliding. This modeling strategy enhanced both the accuracy and manageability of the simulation. A key benefit of this method is the modularity it offers: it allows for the independent modification of either the support components or the main frame, thereby facilitating efficient updates and further numerical investigations.

Load application varied depending on the region of interest. In addition to standard force and pressure loads, zero-dimensional RBE3 elements were used to distribute loads across nodes without introducing unrealistic additional stiffness to the model. The primary suspension system, functioning as the interface between the wheelset and the bogie frame, was modeled using one-dimensional spring elements named CBUSH, as shown in Fig. 2. Capturing the behavior of this subsystem accurately was critical to ensure a realistic representation of the mechanical connection, and to avoid the implementation of overly stiff constraints that could artificially amplify stress concentrations and distort simulation results. The axle and the pin seat were modeled using beam elements with consistent cross-sections. The conical rubber-metal suspension was represented by a pair of one-dimensional spring elements, each linked to the support points through rigid RBE3 multi-node elements, enabling proper load transfer while maintaining the physical fidelity of the assembly. For all load scenarios, boundary conditions were defined by an isostatic scheme, using the four wheel contact points at the ends of the axle as fixed references. The complete FE model comprised about 600,000 elements and 700,000 nodes, achieving an optimal trade-off between model fidelity, mechanical response under loading, result accuracy in terms of displacement and stress, and computational time.

2.3 Optimization settings

The topological optimization performed on the metro bogie frame in this study aimed to develop an innovative structural design tailored for sand casting manufacturing. To achieve this, specific technological constraints were incorporated into the optimization setup, guiding the algorithm toward solutions compatible with casting requirements. The optimization was carried out using commercial software, with the gradient-based method employed as the solving algorithm. All input parameters for the analysis were user-defined, while the solution process was executed automatically by the software. The methodology followed was based on the gradient-based optimization method [27].

The objective of the optimization process was to minimize the weighted compliance across all defined load cases. Compliance, which represents the total strain energy in the mechanical model, serves as an inverse measure of stiffness; higher compliance values indicate greater deformation under load. Minimizing this parameter allows for a more efficient and mechanically robust design outcome. Prior to initiating the optimization, the bogie frame model was modified to better accommodate the solver requirements. In particular, the frame volume was increased and its geometry simplified using basic shapes, granting the optimizer greater design freedom. These modifications were constrained within dimensional limits consistent with the original mechanical components. A critical aspect of the setup was the definition of design and non-design spaces. The design space refers to the regions where the optimizer is permitted to modify the geometry, while the non-design space includes all areas that must remain unchanged due to functional or integration requirements. The latter typically encompasses load application points, connection zones with other components, and interfaces with supporting systems (see Fig. 3). Preserving these interfaces allowed for independent modification of the main frame without affecting the connection to other subsystems.

An optimization constraint was applied in the form of a mass fraction limit, defined as the ratio between the final and initial mass of the design space, which was set to remain below 40%. This is a commonly used threshold in topological optimization, consistent with industrial practice. In order to reflect the inherent symmetry of the bogie structure, a pattern grouping condition was introduced, enforcing mirror symmetry with respect to a midplane normal to the y-axis. This was particularly important given the asymmetric application of loads on the model. After iterative testing, the minimum feature size parameter was set to 20 mm to ensure adequate geometric resolution in the final design. Additionally, the “draw single” constraint was employed to enforce unidirectional material removal, simulating the extraction of the component from a mold and resulting in a geometry that opens toward the specified direction, either upward or downward, depending on the configuration.

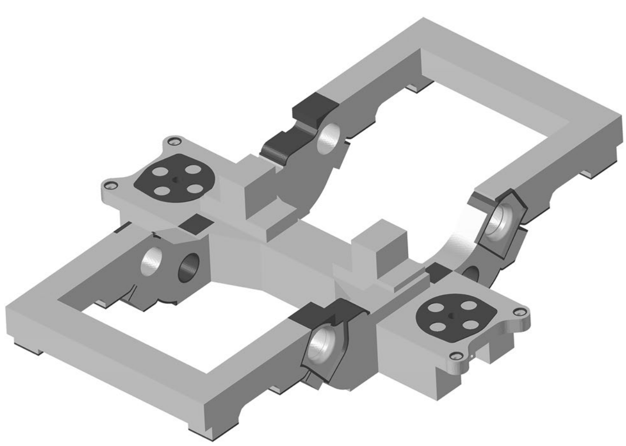

Fig. 3 Bogie frame model to be optimized with distinction between design space (gray) and non-design space regions (black)

2.4 Fatigue

Mechanical fatigue represents a critical issue within railway engineering, particularly concerning components such as bogies, which are subjected to cyclic loading during service. This phenomenon, characterized by the progressive degradation of material properties under repeated stress cycles, plays a pivotal role due to its direct implications on the safety, operational reliability, and maintenance planning of railway systems. The recurrent mechanical stresses experienced throughout operational cycles may initiate microcracks, which, if left unchecked, can propagate and culminate in structural failure. Documented instances of fatigue-induced catastrophic failures, including derailments [28], underscore the necessity for a comprehensive understanding and proactive mitigation of this degradation mechanism.

Incorporating fatigue considerations at the earliest stages of design, maintenance scheduling, and inspection strategies offers a viable means to substantially enhance system durability and reduce accident risk. The current engineering paradigm increasingly emphasizes early-stage component optimization, wherein the integration of fatigue analysis emerges as an indispensable element. Neglecting the influence of cyclic loading during this phase may result in structurally deficient configurations, thereby compromising both reliability and longevity.

By embedding fatigue resistance within the optimization framework, the resulting designs can fulfill not only performance and operational criteria but also exhibit extended service life and minimized maintenance requirements, objectives that align closely with the broader imperatives of sustainability and cost-efficiency in contemporary railway engineering.

Mechanical fatigue refers to the progressive structural degradation of materials subjected to cyclic loading, often occurring at stress levels below the material yield strength. The fatigue phenomenon typically evolves through three distinct phases: initiation of microcracks, frequently located at surface imperfections or geometrical discontinuities; propagation of the crack, evidenced by characteristic features such as striations or beach marks; and ultimate failure, which ensues once the crack reaches a critical dimension. The evaluation of fatigue life is commonly conducted via stress–life cycle (S–N) curves, which establish the correlation between stress amplitude and the number of cycles to failure. Alternatively, fracture mechanics approaches, including Paris' law, are employed to predict crack growth behavior.

In the context of railway engineering, components such as bogies and axles are recurrently exposed to dynamic and fluctuating loads, rendering fatigue a primary design consideration. The phenomenon is further modulated by a combination of environmental conditions, applied stress levels, and inherent material properties. Accordingly, the integration of fatigue assessment into both the design phase and maintenance protocols is essential to ensure structural integrity, operational reliability, and long-term safety.

The selection of an appropriate methodology for fatigue assessment is of paramount importance, as it directly impacts both the components capability to endure throughout its intended service life, bearing significant implications for safety, and its ability to successfully meet certification requirements. Accordingly, it is essential to employ an approach that is not only compliant with established industry standards but also demonstrably ensures structural integrity and operational reliability. The present investigation focuses on railway bogie frames, which are particularly susceptible to fatigue-related damage due to their exposure to variable and cyclic loads. The following sections of this work will examine this specific application in detail. Nevertheless, the general methodology described herein retains applicability to a broader range of structural components, as the proposed approach can be adapted to other applications with minor modifications.

Fatigue assessment in the railway sector is governed by a comprehensive framework of standards, including EN 15827 [29], EN 15085–3 [30], EN 10210 [31], EN 10025 [32], EN 10083 [33], EN 17149 [34], ERRI B 12/RP 17 [35], and ERRI B 12/RP 60 [36]. Among these, EN 13749 constitutes the principal reference for the structural verification of bogie frames, delineating a four-stage evaluation process comprising analytical calculations, static testing, fatigue testing, and on-track validation. Owing to the complexity inherent in fatigue phenomena, responsibility for the detailed analysis is frequently delegated to the supplier, who possesses the requisite technical expertise. Fatigue evaluation may be conducted through two principal methodologies, contingent upon agreement with the client: the fatigue limit-based method and the damage accumulation approach. The former postulates that a material subjected to cyclic loading below a threshold amplitude, denoted as the fatigue limit σ_{FL}, may theoretically sustain an infinite number of cycles without failure. For many ferrous and selected non-ferrous alloys, this endurance limit is empirically derived from Wöhler (S–N) curves. Should the alternating stress σ_a exceed σ_{FL}, fatigue life N can be estimated using Basquin equation:

$$\sigma_a = A \cdot N^b, \tag{1}$$

where A and b are material-specific parameters determined through experimental characterization. In scenarios involving non-zero mean stress, the Goodman–Smith diagram offers a practical and widely accepted means of assessing the combined effects of alternating and mean stress components. The Damage Accumulation Approach, based on the Palmgren–Miner criterion, is particularly suitable for applications involving variable amplitude loading. This method assumes that fatigue damage accumulates across different stress amplitudes and is expressed as

$$D = \sum_i \frac{n_i}{N_i}, \tag{2}$$

where n_i is the number of load cycles applied at stress level $\sigma_{a,i}$, and N_i is the corresponding fatigue life. Structural failure is anticipated when the cumulative damage D reaches or exceeds unity ($D \geq 1$). This approach is indispensable when dealing with irregular or multi-modal loading spectra. The relevant standards stipulate that Wöhler curves must be defined with a survival probability of at least 95%, preferably 97.5%. Provided that the loading scenarios and fatigue data are complete and statistically representative, as required by the standards, these fatigue assessments may be performed without the inclusion of supplementary safety factors. Appendix E of EN 13749 outlines the prescribed analytical procedures, which are fundamental in addressing fatigue-related challenges. Moreover, the standard mandates that loading cases account for the full spectrum of operational conditions, thereby reducing parametric uncertainty, and strongly advocates for the application of numerical methods such as finite element analysis (FEA). When an infinite fatigue life is the intended design objective, preference is generally given to the fatigue limit-based methodology.

2.5 Assessment of fatigue under multiaxial loading

In railway vehicles, and consequently in bogie frame structures, multiaxial stress states are frequently encountered. While EN 13749 addresses the structural assessment of bogies, it does not prescribe a specific methodology for the evaluation of multiaxial fatigue. Instead, Appendix F of the standard states that the procedure for dealing with multiaxial stress conditions must be defined within the technical specification, effectively delegating the methodological choice to the design engineer. In this study, the procedure described in ERRI B 12/RP 60, which builds upon the framework established in ERRI B 12/RP 17, has been adopted. These technical reports were developed by the European Railway Research Institute (ERRI), formerly the Office for Research and Experiments (ORE), prior to its dissolution in 2005.

The methodologies presented therein, together with the UIC Fiches, have since been assimilated into the current body of European standards.

Appendix G of ERRI B 12/RP 60 provides specific guidance for determining fatigue limit stresses under multiaxial loading conditions. It is generally recognized that upon initiation, a crack tends to propagate perpendicularly to the direction of the maximum tensile principal stress. The adopted procedure is based on identifying this critical orientation, referred to as the "preferred direction," and evaluating the fatigue-relevant variations of the normal stress component in that direction. The methodology comprises the following sequential steps, to be applied at each finite element or nodal point in the structural model, as shown in Fig. 4:

1. Computation of the stress tensor for each element or node under every defined load case. The stress tensor characterizes the internal force distribution resulting from applied external loads. For the i-th loadcase (LCi) the following tensor can be calculated:

$$\boldsymbol{\sigma}^{\mathrm{LC}i}_{XYZ} = \begin{bmatrix} \sigma^{\mathrm{LC}i}_{xx} & \sigma^{\mathrm{LC}i}_{xy} & \sigma^{\mathrm{LC}i}_{xz} \\ \sigma^{\mathrm{LC}i}_{yx} & \sigma^{\mathrm{LC}i}_{yy} & \sigma^{\mathrm{LC}i}_{yz} \\ \sigma^{\mathrm{LC}i}_{zx} & \sigma^{\mathrm{LC}i}_{zy} & \sigma^{\mathrm{LC}i}_{zz} \end{bmatrix}, \tag{3}$$

   where $\sigma^{\mathrm{LC}i}_{xx}$, $\sigma^{\mathrm{LC}i}_{yy}$, and $\sigma^{\mathrm{LC}i}_{zz}$ represent the normal stresses along the respective directions; $\sigma^{\mathrm{LC}i}_{xy}$, $\sigma^{\mathrm{LC}i}_{xz}$, $\sigma^{\mathrm{LC}i}_{yz}$ and their respective counterparts represent the shear stresses acting on the respective planes.

2. Determination of the principal stresses ($\sigma^{\mathrm{LC}i}_{xx\mathrm{P,LC}i}, \sigma^{\mathrm{LC}i}_{yy\mathrm{P,LC}i}, \sigma^{\mathrm{LC}i}_{zz\mathrm{P,LC}i}$) and their respective directions $\left(\widehat{X_{\mathrm{P,LC}i}}, \widehat{Y_{\mathrm{P,LC}i}}, \widehat{Z_{\mathrm{P,LC}i}}\right)$ for each load case. The principal components of the stress tensor are determined by solving the characteristic equation derived from its determinant:

$$\det(\boldsymbol{\sigma} - \lambda \boldsymbol{I}) = 0. \tag{4}$$

   The eigenvalues correspond to the principal stresses, i.e., the normal stresses along orientations where shear components vanish $(\sigma^{\mathrm{LC}i}_{xy} = \sigma^{\mathrm{LC}i}_{xz} = \sigma^{\mathrm{LC}i}_{yz} = \sigma^{\mathrm{LC}i}_{yx} = \sigma^{\mathrm{LC}i}_{zx} = \sigma^{\mathrm{LC}i}_{zy} = 0)$. The eigenvectors identify the principal directions, rendering the stress tensor ($\boldsymbol{\sigma}^{\mathrm{LC}i}_{XYZ}$) diagonal in the transformed reference frame ($X_{\mathrm{P,LC}i}Y_{\mathrm{P,LC}i}Z_{\mathrm{P,LC}i}$):

$$\boldsymbol{\sigma}^{\mathrm{LC}i}_{X_{\mathrm{P,LC}i}Y_{\mathrm{P,LC}i}Z_{\mathrm{P,LC}i}} = \begin{bmatrix} \sigma^{\mathrm{LC}i}_{xx\mathrm{P,LC}i} & 0 & 0 \\ 0 & \sigma^{\mathrm{LC}i}_{yy\mathrm{P,LC}i} & 0 \\ 0 & 0 & \sigma^{\mathrm{LCi}}_{zz\mathrm{P,LC}i} \end{bmatrix}. \tag{5}$$

3. Determination of the maximum principal stress ($\sigma_{\max}$, corresponding to $\sigma^{\mathrm{LCK1}}_{yy\mathrm{P,LCK1}}$), identified as the highest between the algebraic values of all the principal stresses of all loadcase and its corresponding direction ($\widehat{Y_{\mathrm{P,LCK1}}}$).

4. Projection of the stress tensors from all remaining load cases (excluding the one responsible for $\sigma_{\max}$, namely $\boldsymbol{\sigma}^{\mathrm{LCK1}}_{XYZ}$) onto the direction of $\sigma_{\max}$ ($\widehat{Y_{\mathrm{P,LCK1}}}$ in the example of Fig. 1):

$$\sigma^{\mathrm{LC}i}_{\mathrm{projected}} = \widehat{Y_{\mathrm{P,LCK1}}} \cdot \boldsymbol{\sigma}^{\mathrm{LC}i}_{XYZ} \cdot \widehat{Y_{\mathrm{P,LCK1}}}. \tag{6}$$

   This scalar projection is mathematically performed by double contracting the stress tensor with a unit vector aligned with the direction of the maximum principal stress ($\widehat{Y_{\mathrm{P,LCK1}}}$) and represents the magnitude of the stress component (of the tensor $\boldsymbol{\sigma}^{\mathrm{LC}i}_{XYZ}$) acting along that orientation.

5. Determination of the minimum stress value ($\sigma_{\min}$) generated by any of the projected load cases. In the example of Fig. 4, the minimum is generated by projection of the tensor induced by K2 loadcase (LCK2):

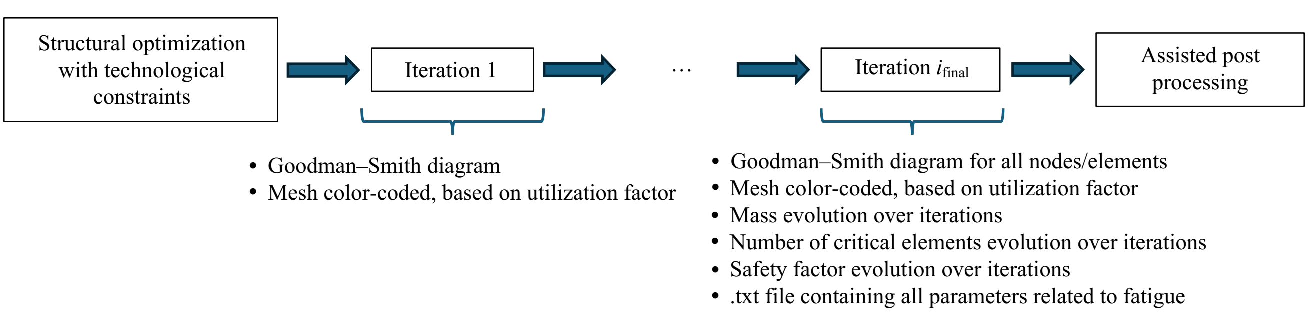

Fig. 4 Calculation of fatigue under multiaxial stress conditions

$$\sigma_{\min} = \sigma^{\text{LCK2}}_{\text{projected}}. \tag{7}$$

6. Calculation of the mean stress (σ_{mean}) and stress amplitude ($\Delta\sigma$) as follows: $\sigma_{\text{mean}} = (\sigma_{\max} + \sigma_{\min})/2$ and $\Delta\sigma = (\sigma_{\max} - \sigma_{\min})/2$. In the considered example, the situation is as follows:

$$\sigma_{\text{mean}} = \frac{\sigma^{\text{LCK1}}_{yy\text{P,LCK1}} + \sigma^{\text{LCK2}}_{\text{projected}}}{2}, \tag{8}$$

$$\Delta\sigma = \frac{\Delta^{\text{LCK1}}_{yyP,\text{LCK1}} - \sigma^{\text{LCK2}}_{\text{projected}}}{2}. \tag{9}$$

This procedure provides a robust and technically sound basis for assessing fatigue-relevant stress fluctuations in the most critical orientation, thereby enhancing the predictive accuracy of fatigue evaluations in multiaxial loading scenarios.

2.6 Methodology

The methodological framework employed for the redesign of the metro bogie frame integrates computer aided design (CAD) modeling, FEA and structural optimization, while systematically incorporating manufacturing constraints specifically associated with the sand casting process and accounting for fatigue-related phenomena. The distinctive aspect and the novelty of this research lies in the systematic integration of fatigue analysis throughout the entire design workflow, thereby ensuring that the final geometry not only satisfies structural performance criteria but is also compatible with manufacturing feasibility requirements. The methodology developed enables the implementation of several fundamental capabilities:

1. The automated assessment of fatigue life for a given geometry, facilitating acceptance or rejection based on fatigue strength criteria by detecting finite elements exhibiting safety factors below unity and graphically representing their performance through Goodman–Smith diagrams.
2. The capability to monitor, at each iteration, the quantity and spatial distribution of critical elements exceeding fatigue thresholds, thereby allowing for the identification of correlations between specific geometric characteristics and/or mass distribution and the corresponding fatigue performance, as inferred from the evolution of geometry and mass allocation throughout the optimization sequence.
3. The incorporation of fatigue-driven design modifications during the reconstruction phase of the final optimized topology, capitalizing on the established relationships between material distribution patterns and fatigue response. The development of a bogie frame geometry amenable to sand casting, a solution that constitutes a significant advancement within the context of railway engineering. Conventionally, bogie frames are fabricated using structural steel and assembled through welding techniques, primarily due to the inherent geometric complexity of such components. The methodology herein proposed departs from this established paradigm by facilitating the adoption of castable materials, without compromising structural performance or mechanical reliability. In order to enable a comprehensive and realistic evaluation of the optimized design, the mechanical properties of a selected cast material were explicitly integrated into the numerical simulations. Specifically, the chosen reference material was EN-GJS-450–10, whose mechanical characteristics are detailed in [37].
4. The extension of the earlier work conducted by A. Cascino [38], which was originally confined to static stress evaluations, through the systematic inclusion of fatigue considerations. In particular, this study undertakes a comparative analysis of fatigue life evolution within optimization procedures based on critical loading conditions, identified via sensitivity analysis, versus those employing the full spectrum of prescribed loads. The objective is to determine the continued validity of the sensitivity-based methodology in the presence of fatigue constraints, thereby yielding valuable insights into the robustness and applicability of such optimization strategies under cyclic loading conditions.

In order to accomplish the previously described tasks, a batch file was developed to ensure compatibility with any geometry and application. This file generates a wide range of results that, after careful interpretation by the designer, facilitate the execution of all required analysis.

The procedure begins by prompting the user to input key parameters, including the.fem file name, fatigue analysis frequency, and a minimum density threshold for topology refinement. After setting up the required directories, a Python script extracts element centroids from the.fem file. The model is then analyzed using a FE solver. The resulting optimization output is parsed to identify the final iteration, ensuring fatigue evaluation occurs at the last step regardless of user-defined intervals. Scripts are employed to generate plots of mass evolution and to compute fatigue life for elements exceeding the density threshold, using stress data from the solver. The results, including detailed stress metrics and centroid locations, are saved in.csv and text formats for compatibility with FE software. Finally, visualization scripts produce Goodman-Smith diagrams and color-coded mesh images, illustrating element-wise utilization across iterations.

One of the most significant challenges in writing the Python scripts was handling the massive dataset sizes. With the aim to mitigate memory limitations, the scripts were optimized to write output progressively rather than storing intermediate results in variables before writing them to output files. Moreover, for efficient reading of large files, a chunk-based processing method was implemented to enhance performance and reduce memory overhead.

Following the execution of the batch routine, a series of key outputs are produced, providing the foundation for subsequent analysis and interpretation, as summed up into Fig. 5. These include:

- The evolution of mass across iterations, which serves as a critical indicator for monitoring the progress and effectiveness of the optimization process.
- Goodman–Smith diagrams generated for each iteration, illustrating all critical elements that exceed fatigue limits. These plots enable the identification of elements failing to meet safety requirements and allow differentiation between exceedances due to excessive mean stress or alternating stress. Comparative analysis of these diagrams across successive iterations provides valuable insights into the progression of fatigue behavior throughout the optimization.
- Three-dimensional mesh visualizations for each iteration, wherein elements are color-coded according to their utilization factor. Examination of the final iteration alone facilitates the localization of geometrically critical regions requiring refinement, while the comparison of multiple iterations enhances the understanding of fatigue behavior development over time.
- The evolution of the safety factor for individual elements across all iterations. When combined with the aforementioned 3D visualizations, this information supports the identification and tracking of structurally critical regions, thereby allowing for the correlation of topological modifications with changes in fatigue performance. Analyzing the interplay between mass redistribution and the temporal trend of safety factors provides a valuable basis for refining the design and mitigating fatigue-related vulnerabilities.

The proposed methodology is deliberately structured to support comprehensive fatigue investigations, as the generated outputs extend well beyond the scope strictly necessary for the present study. Moreover, both the Python scripts and the batch file have been developed with modularity and flexibility in mind, thereby enabling users to introduce additional result types, integrate alternative fatigue assessment models, and tailor output formats to specific analytical requirements.

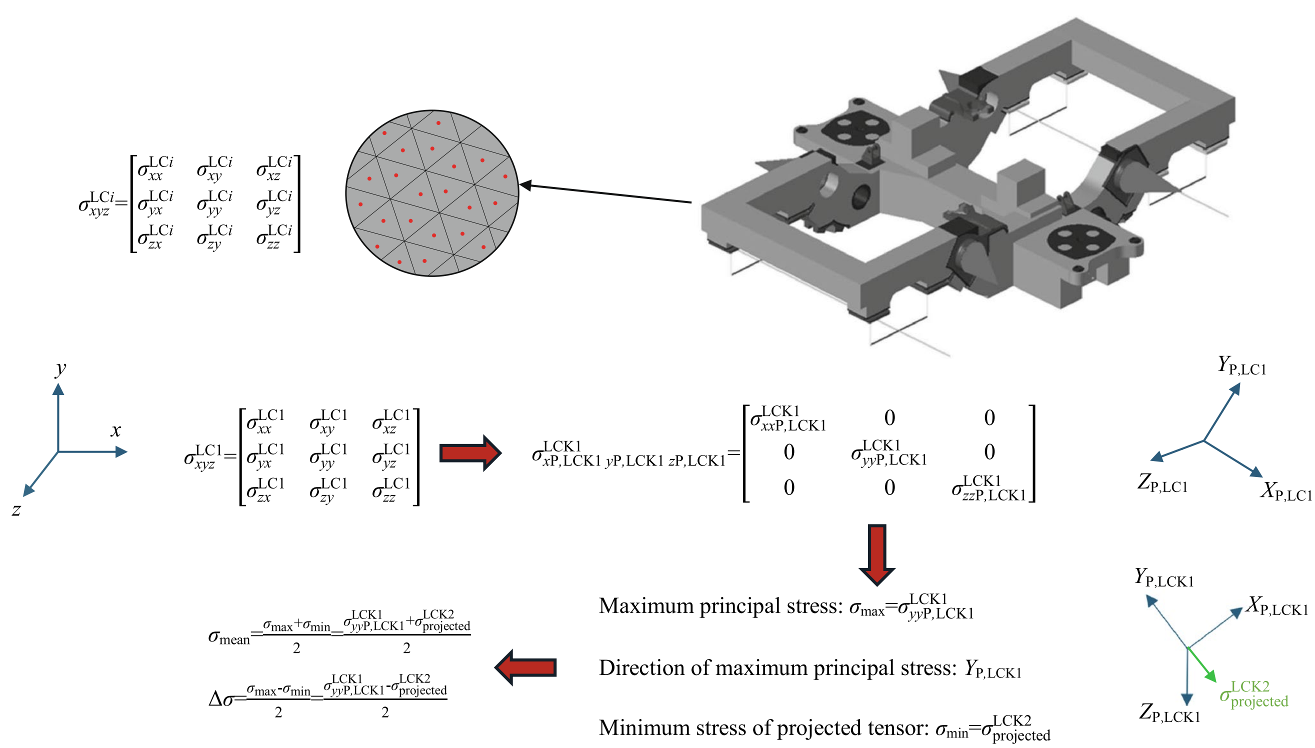

Fig. 5 Methodology workflow

3 Results and discussion

3.1 Methodology application: optimization process analysis

As an initial application of the proposed methodology, the evolution of fatigue behavior throughout the optimization process has been investigated.

In the analysis presented below, both the geometries and the associated results from iterations preceding the third are deliberately excluded, with the exception of iteration 0, which corresponds to the initial geometry. This omission is justified by the non-physical material distribution observed in the early stages of the optimization, which is characterized by a significant presence of disconnected or sparsely populated elements. This behavior is primarily attributed to the solver's initial tendency to assign extremely low-density values to a large subset of elements. Given that elements with density values falling below a predefined threshold are systematically excluded from structural evaluation, the resulting configurations during these early iterations exhibit discontinuous and fragmented geometries that do not reflect realistic structural behavior. Moreover, iterations 4 and 7 have also been excluded from the analysis, as they do not demonstrate any reversal or deviation in the trend concerning the number of critical elements, which in the present study are defined as those exhibiting a utilization factor exceeding unity. This trend is quantitatively illustrated in Fig. 6, where red columns indicate the analyzed iterations and light blue columns indicate the unexamined ones, and it serves as a reference metric for assessing the temporal progression of fatigue-critical regions throughout the optimization sequence.

At iteration 0, a total of 13 critical regions were identified. Among these, 12 are located within or in the immediate vicinity of the non-design domain, a distribution primarily attributed to the fact that optimization constraints are applied exclusively within the design space and are limited to static stress conditions. Since fatigue evaluation is conducted through combinations of static stress states, regions subjected to elevated static loads tend to exhibit increased peak stress amplitudes, thereby experiencing greater fatigue demand. This behavior is consistently observed in subsequent iterations. Future investigations may consider the inclusion of fatigue-related constraints within the non-design space to mitigate this effect. The emergence of critical zones is primarily associated with specific geometric features. In particular, six regions located at the primary suspension attachment points correspond to sharp geometrical discontinuities adjacent to chamfered holes. Four additional zones, situated at the attachment interfaces of the braking support system, exhibit similar features in the form of sharp edges near chamfered protrusions. The support structure of the reducer, functioning as a cantilevered extension, is subjected to high mechanical loads. Lastly, an additional critical region is detected at the terminus of the gooseneck, characterized by an unfilleted edge.

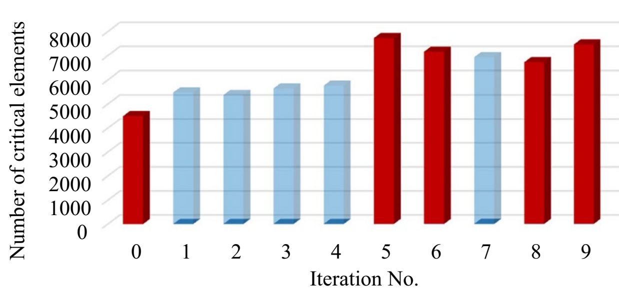

Fig. 6 Trend in the number of critical elements across all iterations, with analyzed iterations shown in red and iterations pending examination in light blue

At iteration 5 the aforementioned critical regions persist, although involving a greater number of elements. Furthermore, new critical areas emerge due to insufficient filleting and reduced material accumulation at the intersection of the transverse and longitudinal beams, which result in elevated local stress concentrations. Additional criticalities are identified in the central transverse beams, where sharp geometrical transitions and significant material deficits are present. The lower region of the bogie also presents several critical zones due to step-like features and inadequately dimensioned fillet radii. These developments culminate in a notable increase in the number of critical elements, from 4492 at iteration 0 to 7718 at iteration 5.

At iteration 6, a reduction in critical elements is observed, decreasing to 7151. The removal of certain non-filleted edges suggests that the redistribution of material, although not explicitly driven by fatigue criteria, has led to an unintended enhancement in fatigue performance. A logical extension of this approach would be the deliberate imposition of targeted constraints to replicate such improvements systematically.

Between iterations 6 and 8, the number of critical elements continues to decrease, reaching 6712. This reduction is attributed to the disappearance of four previously critical zones due to improved material placement beneath the central beam. Nonetheless, two new critical regions are identified: one characterized by an inadequately rounded fillet, and another by a sharp edge.

At iteration 9 (Fig. 7), a slight increase in the number of critical elements is noted, although iteration 5 remains the most critical in terms of overall fatigue demand. No new critical zones are observed; however, existing ones exhibit spatial expansion. In addition to geometrical refinements, the

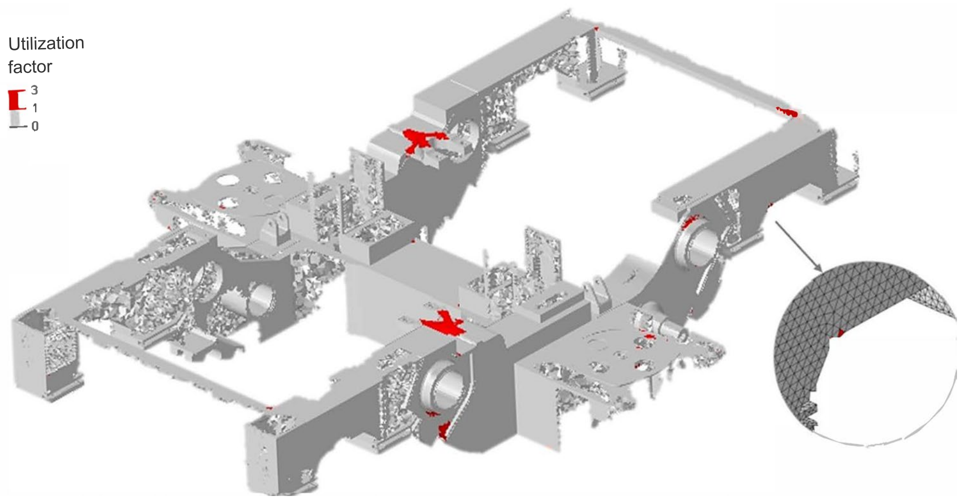

Fig. 7 Mesh color-coded, based on utilization factor at iteration 9

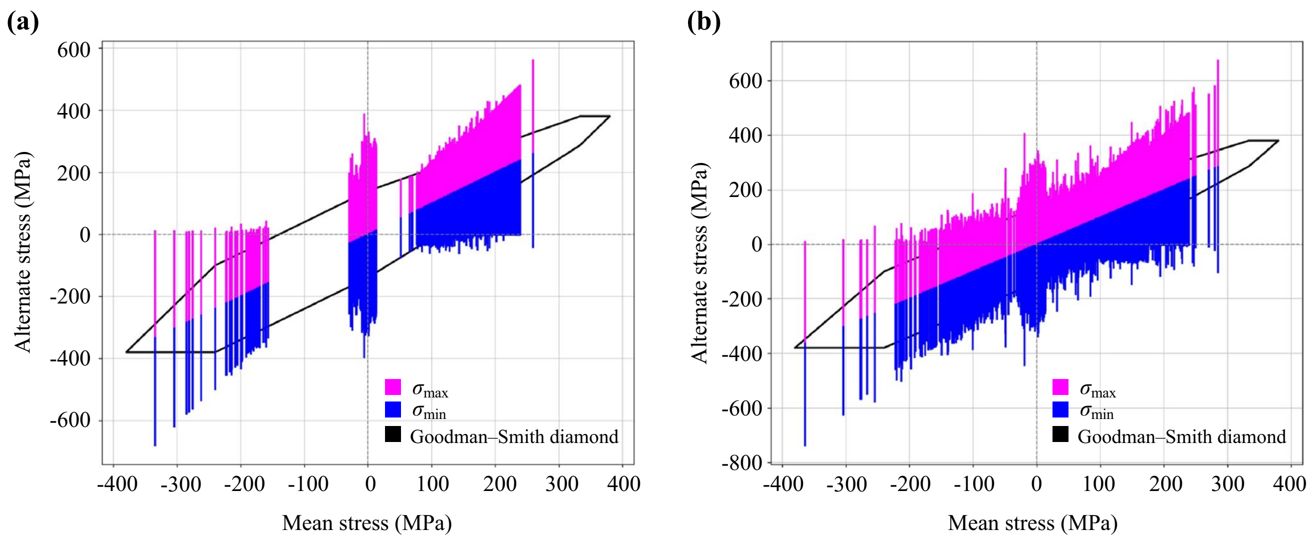

Fig. 8 Comparison of Goodman–Smith diagram: **a** iteration 0; **b** iteration 9

evolution of mass distribution exerts a substantial influence on fatigue behavior.

Further insights into the fatigue behavior are provided by the Goodman–Smith diagrams shown in Fig. 8, which display the fatigue data of all critical elements across iterations. The lines represent stress range amplitudes ($\Delta\sigma$), with fuchsia segments denoting σ_A (to be added to σ_{mean} to obtain σ_{max}) and blue segments corresponding to σ_{min}. At iteration 0, element distribution is concentrated around $\sigma_{mean} \approx 0$ and $\sigma_{mean} > 100$ MPa, whereas in the final iteration, the distribution is more uniform. Elements with the lowest safety factors, i.e., those whose reference line extremes extend well beyond the Goodman–Smith fatigue limit diamond, are located at both high σ_{mean} and near-zero σ_{mean}. A clear trend is observed: as σ_{mean} increases, σ_A also increases, leading to progressively higher $\Delta\sigma$ values. This trend, combined with the tightening of admissible $\Delta\sigma$ ranges at high σ_{mean}, results in extremely low safety factors at elevated mean stress levels——a pattern that is not evident at iteration 9.

3.2 Methodology application: geometry reconstruction

This section demonstrates the application of the developed methodology to reconstruct the post-optimization geometry with explicit consideration of fatigue. Indeed, the geometry obtained in the final iteration of the optimization process must be modified by the designer to ensure manufacturability, simplify the design and meet other practical requirements. It should be noted that although casting-oriented

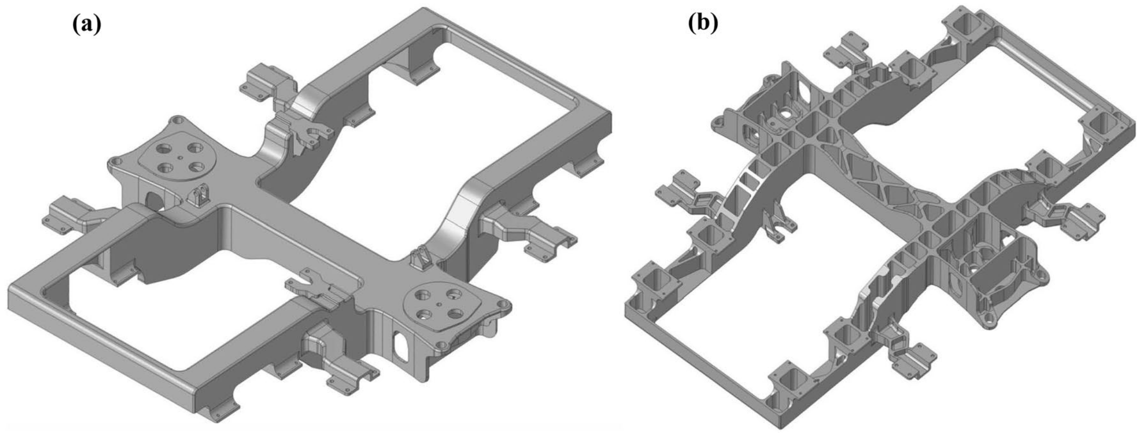

Fig. 9 Geometry reconstruction without fatigue influence: **a** last iteration; **b** reconstructed geometry

constraints were already included in the optimization setup, the numerical output nonetheless necessitates a manual reconstruction phase. This step is necessary to obtain a smooth, manufacturable CAD geometry and is a standard practice in topology optimization workflows.

To illustrate the added value of the methodology, a reconstruction of a geometry based solely on technological considerations is presented and the associated fatigue issues, which could have been avoided using the proposed methodology, are highlighted. The reconstruction process (Fig. 9) commenced with the central crossbeam, followed by the two longitudinal beams, and concluded with the integration of supports and various interface regions. To simplify manufacturing, the lower section of the frame was designed as an open structure. This design eliminates the need for cores in the main structure, which would have been costly due to the frame dimensions. However, some cores were necessary around the secondary suspension areas, as illustrated in the subsequent figures. Reinforcement elements were introduced throughout the lower section to enhance stiffness and resistance to both bending and torsion while also ensuring a uniform molten metal flow during casting.

Additionally, the open-bottom design, oriented toward the rail, prevents the accumulation of external agents that could damage the metal structure. Several supports, not initially considered in the optimization geometry, were included in the final design to ensure the producibility of the entire frame within the same casting process. The computational procedures described in previous sections were applied to this design. The number of elements exhibiting a safety factor below 1 was 6771, most of which were located in the support regions, which were not subjected to optimization. These areas are likely critical because they belong to the non-design space, where stress constraints were not imposed during optimization. In addition to the supports, critical elements were found at fillet transitions, as expected.

Even when excluding the supports, the presence of critical elements indicates that this design is not fatigue-safe, as fatigue is a localized phenomenon. The most relevant

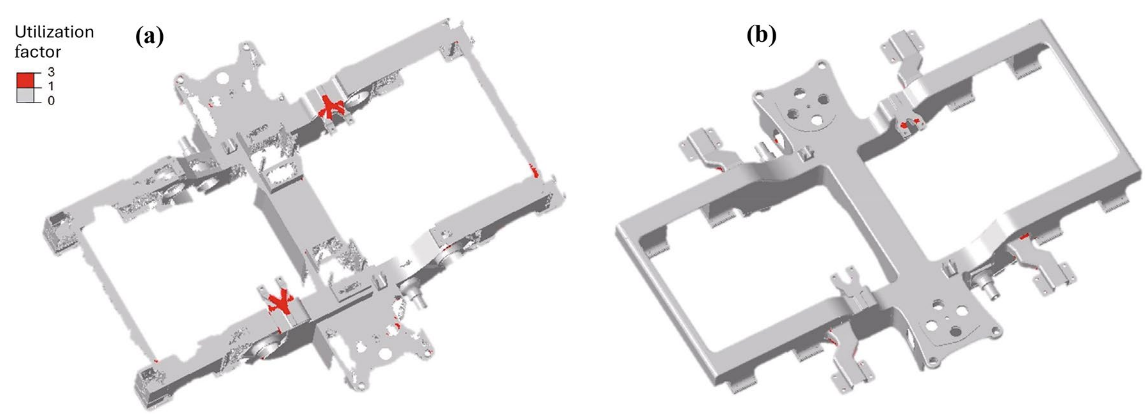

Fig. 10 Comparison of critical areas in **a** the last iteration and in **b** the final geometry reconstructed based upon technological considerations

finding, illustrated in Fig. 10, is that the critical areas identified in the last optimization iteration recur in the final geometry, since the reconstruction was carried out based solely on technological considerations. Consequently, the final geometry obtained solely through such considerations could have been fatigue-compliant if the proposed methodology had been applied, as the designer would have noticed the fatigue issues earlier and would not have repeated them in the final design.

The novelty of this study lies in utilizing fatigue analysis to guide the final geometry reconstruction. After topology optimization, a reconstruction phase is always required, which, even when partially assisted by software, is ultimately performed by the designer. The methodology introduced in this work allows for geometry reconstruction that incorporates fatigue performance alongside technological considerations. This approach offers significant advantages, as it ensures a final design that meets fatigue criteria without increasing the overall design time, given that the reconstruction phase is necessary in any case.

3.3 Methodology application: sensitivity analysis

This section revisits the findings reported in reference [38]. The referenced study identified the most critical load cases through a sensitivity analysis and subsequently conducted a topology optimization based on this reduced load set. A parallel optimization was also performed considering the full set of load cases. The results revealed a high degree of similarity between the topologies obtained from both approaches, ultimately leading to the same reconstructed geometry. Accordingly, the final design derived from either optimization pathway was found to be identical, thereby demonstrating that a reduced load set may be used without compromising the outcome. This reduction translated into a 57% decrease in computational time.

The present study extends this investigation to determine whether similar equivalence holds when fatigue behavior is also considered. Given that reference identified the most influential load cases for static conditions, it is plausible that these may not coincide with the most critical cases under fatigue loading. If this is confirmed, then different critical regions may emerge in the resulting geometries from the two optimization strategies. The principal aim of the current investigation is to confirm whether the final geometry, reconstructed with both technological and fatigue considerations in mind, remains consistent across both optimization approaches (with and without sensitivity analysis). Should discrepancies arise, this would imply that applying sensitivity analysis based on static stress alone is inadequate for design workflows where fatigue compliance is a primary objective.

An analysis of the data presented in Fig. 11 reveals a substantial difference in the number of critical elements between the two optimization scenarios.

The number of critical elements exhibits an inverse correlation with the trend of mass reduction, with the sole exception of the transition between iterations 1 and 2. Overall, the optimization process results in a marked deterioration of fatigue performance. This degradation is primarily attributed to the following factors:

1. a substantial reduction in total mass, from 4300 to 1390 kg, which inherently affects structural stiffness and alters load paths;
2. the presence of geometrical features, such as sharp edges, which do not compromise static performance and

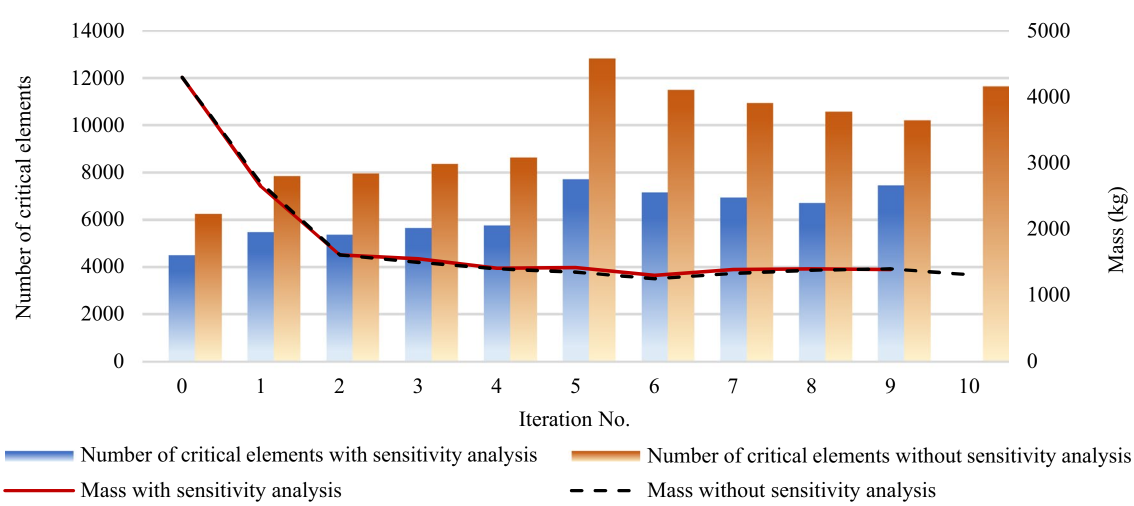

Fig. 11 Trend of the mass and number of critical elements over the iterations, with and without sensitivity analysis

were consequently not constrained during the optimization phase; and

3. stress intensifications induced by mesh discretization. Specifically, coarse meshing generates numerical stress concentrations, an issue that is addressed in the reconstruction of the final geometry through the smoothing of irregular surface features.

It can be observed that the mass remains almost identical between the two test configurations during the optimization process, while the number of critical elements differs from the beginning. This leads us to the following observations:

First, the correlation between mass evolution and the number of critical elements can be discussed by distinguishing two ranges: from iteration 0 to iteration 5, and from iteration 5 onward. In the first range, characterized by a sharp mass reduction, a justified increase in the number of critical elements is observed. This behavior can be explained by the solver aggressively removing material in order to satisfy the imposed constraint, which consequently deteriorates the fatigue performance of the frame. The effect is particularly evident in the case without sensitivity analysis. From iteration 5, a peak in the number of critical elements occurs, followed by a further decrease in mass until a minimum is reached at iteration 10, after which a slight increase is observed. In conclusion, the mass reduction is strongly correlated with the increase in critical elements in the initial phase of the optimization process, while the correlation becomes weaker in the later phase.

Second, it is important to note that in terms of material distribution, as shown in Fig. 12, the two solutions are practically equivalent. For this reason, the presence of a larger number of and variety of load conditions could lead to an increase in the number of critical elements in more localized areas. Therefore, the search for an optimal trade-off between the number of critical elements, the localization of additional critical elements, and the computation time required for the complete analysis could represent an interesting aspect for future development. Further case studies are required to investigate this issue in depth.

A comparison (Fig. 12) of the final iterations—iteration 10 (without sensitivity analysis) and iteration 9 (with reduced load cases)—shows that the critical regions are highly similar, with only two exceptions. However, the

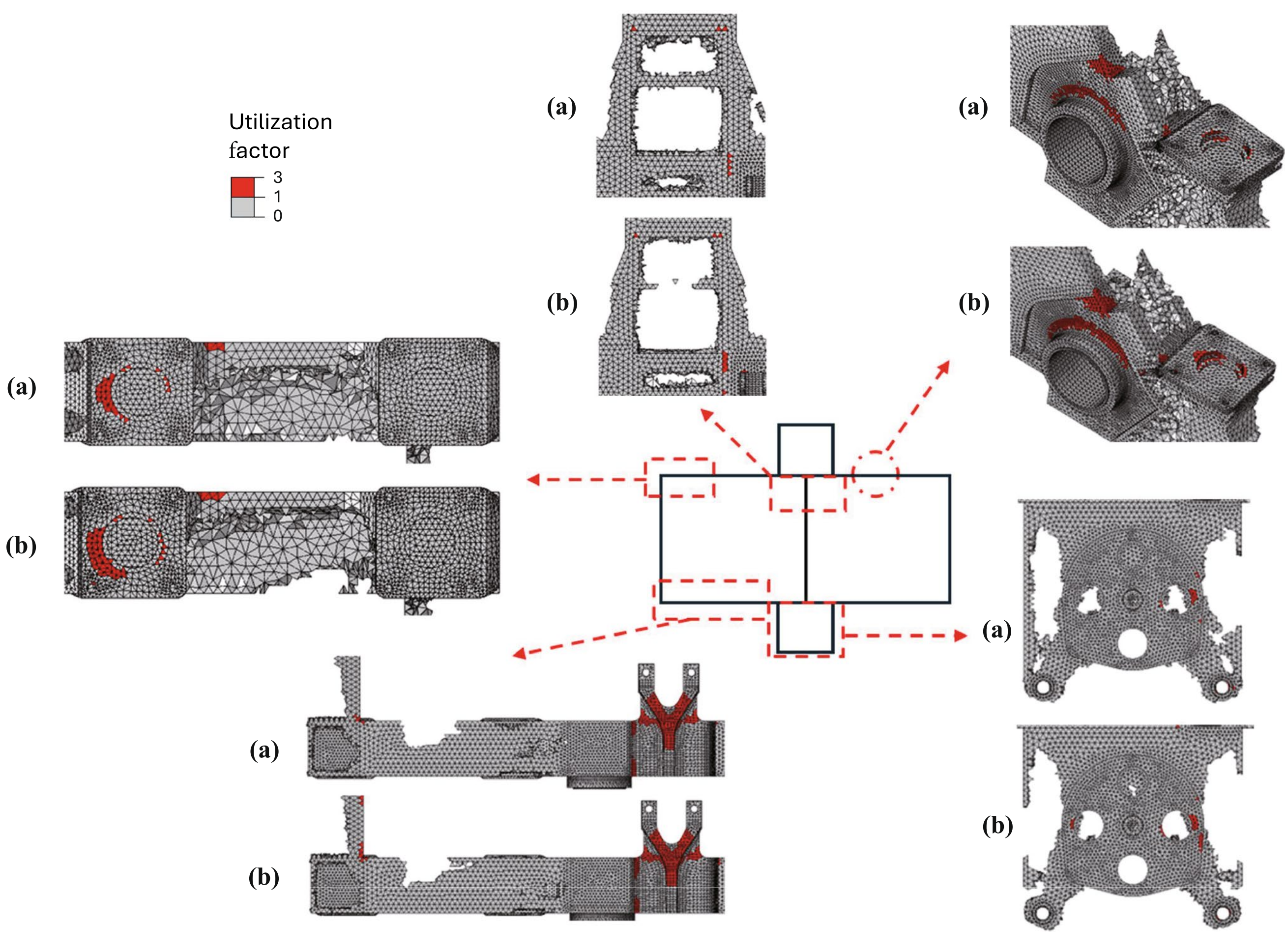

Fig. 12 Final iteration of the optimization **a** without sensitivity analysis and **b** with sensitivity analysis

nature of these two new critical zones is such that they would not influence the reconstruction:

1. The first is located on a perimeter beam. Given that the corresponding beam on the symmetrical side is also critical in the sensitivity-analysis case, and considering that symmetry is a design priority, this region would likely have been addressed during reconstruction regardless of its critical status.
2. The second lies within the non-design space and is therefore unmodifiable.

Consequently, neither of these newly identified critical zones would affect the final geometric reconstruction.

The critical areas relevant to reconstruction matched very well between the two analyses, with only a difference in the number of elements within them. However, once a critical region is modified, it is completely resolved regardless of the number of critical elements it contains. It can therefore be concluded that the reconstructed designs obtained from the final iterations of both optimizations (with and without sensitivity analysis) are identical in terms of fatigue considerations, as the critical fatigue areas requiring modification remain the same. Given all these considerations, it is not possible to determine whether the load cases excluded by the sensitivity analysis (based on static considerations) are influential for fatigue. However, the test case examined demonstrated that the final conditions of both optimizations yield the same final design, as the fatigue-critical areas requiring modification are identical. For this specific test case, applying sensitivity analysis based on static considerations proves beneficial even when fatigue is considered, as it reduces computational time while still producing an identical final geometry with the same fatigue safety level. However, to establish this conclusion as a general rule, further test cases must be analyzed, as the current deductions are based solely on comparative evaluations rather than a fundamental scientific principle.

4 Conclusions and future developments

The present research has developed and applied a dedicated methodology for the automated evaluation of fatigue-related parameters within structural optimization workflows. The approach, implemented through a custom-developed software tool, was designed to interface effectively with major commercial FEA platforms and to generate a wide array of results, thereby ensuring high versatility and adaptability. This, in turn, enhances the efficiency of design innovation processes by streamlining fatigue assessment and enabling more informed, data-driven decisions throughout the optimization cycle.

The proposed methodology was applied to the structural optimization of a metro bogie frame, with fatigue behavior assessed iteratively throughout the optimization process. The overall mass of the frame was reduced by approximately 67%. Although this reduction was fundamental in achieving lightweight design goals, it introduced more severe stress concentrations in specific regions, leading to a general deterioration in fatigue performance over the course of optimization. Specifically, the number of critical elements increased by 72% by iteration 5. A detailed analysis of successive iterations identified key correlations between critical fatigue zones, specific geometric features, mass distribution patterns, and mesh-induced effects.

The methodology was subsequently employed to guide the reconstruction of the final geometry, ensuring both manufacturability and compliance with fatigue resistance requirements. While this stage is typically driven solely by manufacturing constraints, the inclusion of fatigue considerations allowed for the generation of fatigue-resilient designs without increasing overall design effort. Furthermore, a sensitivity analysis was conducted to identify the most critical load cases in terms of static stress, enabling an optimization process based on a reduced set of loading conditions. A comparison between the topologies obtained using the complete and reduced load sets indicated no significant differences in the final designs, in terms of either geometry or fatigue behavior, suggesting the feasibility of this simplification for the present case study. These findings underscore the potential of integrating sensitivity-based strategies into fatigue-oriented optimization.

In conclusion, while the full potential of the proposed methodology remains to be explored, its implementation has proven valuable for enhancing structural optimization processes, especially in facilitating the early-stage assessment of fatigue performance during the design phase.

References

1. Zhang LX, Meng XJ, Ding ZJ et al (2023) Simulation-based reliability design optimization method for industrial robot structural design. Appl Sci 13(6):3776
2. Albers A, Ottnad J (2009) Integrated structural and controller optimization for lightweight robot design. In: 2009 9th IEEE-RAS

International Conference on Humanoid Robots, Paris, France, December 7–10, 2009
3. Guo S, Gao J, Guo J et al (2016) Design of the structural optimization for the upper limb rehabilitation robot. In: 2016 IEEE International Conference on Mechatronics and Automation, Harbin, China, 7–10 August 2016. IEEE, pp 1185–1190
4. Shanmugasundar G, Sivaramakrishnan R, Meganathan S et al (2019) Structural optimization of an five degrees of freedom (T-3R-T) robot manipultor using finite element analysis. Mater Today Proc 16:1325–1332
5. Pietropaoli M, Ahlfeld R, Montomoli F et al (2016) Design for additive manufacturing: internal channel optimization. In: Proceedings of the ASME Turbo Expo 2016: Turbomachinery Technical Conference and Exposition, Volume 5B: Heat Transfer, Seoul, South Korea, 13–17 June 2016
6. Kirsch KL, Thole KA (2018) Experimental investigation of numerically optimized wavy microchannels created through additive manufacturing. J Turbomach 140(2):021002
7. Li Z, Zheng X (2017) Review of design optimization methods for turbomachinery aerodynamics. Prog Aerosp Sci 93:1–23
8. Bandini A, Cascino A, Meli E et al (2024) Improving aeromechanical performance of compressor rotor blisk with topology optimization. Energies 17(8):1883
9. Korta J, Raniolo R, Danti M et al (2012) Multi-objective optimization of a car body structure. SAE Int J Passeng Cars Mech Syst 5(3):1143–1152
10. Leiva JP (2011) Structural optimization methods and techniques to design efficient car bodies. In: Proceedings of International Automotive Body Congress 2011, Troy, Michigan, USA, 9–10 November 2011. Curran Associates, Inc., NY, pp 190–213
11. Christensen J, Bastien C (2015) Nonlinear optimization of vehicle safety structures: Modeling of structures subjected to large deformations. Butterworth-Heinemann, Elsevier
12. Miao BR, Luo YX, Peng QM et al (2020) Multidisciplinary design optimization of lightweight carbody for fatigue assessment. Mater Des 194:108910
13. Cho JG, Koo JS, Jung HS (2016) A lightweight design approach for an EMU carbody using a material selection method and size optimization. J Mech Sci Technol 30(2):673–681
14. Cascino A, Meli E, Rindi A (2025) Comparative analysis and dynamic size optimization of aluminum and carbon fiber thin-walled structures of a railway vehicle car body. Materials 18(7):1501
15. Koenig J (2011) Integral consideration of the lightweight design for railway vehicles. Paper presented at Young Researchers Seminar 2011, Technical University of Denmark, Lyngby, Denmark, 8–10 June, 2011
16. Cascino A, Meli E, Rindi A (2023) Dynamic size optimization approach to support railway carbody lightweight design process. Proc Inst Mech Eng Part F J Rail Rapid Transit 237(7):871–881
17. Cascino A, Meli E, Rindi A (2023) A strategy for lightweight designing of a railway vehicle car body including composite material and dynamic structural optimization. Railw Eng Sci 31(4):340–350
18. Srivastava PK, Shukla S (2021) Topology optimization: weight reduction of Indian railway freight bogie side frame. Int J Mech Eng 6:4374–4383
19. Cascino A, Meli E, Rindi A (2024) Development of a methodology for railway bolster beam design enhancement using topological optimization and manufacturing constraints. Eng 5(3):1485–1498
20. Yamamoto M (2020) Non-parametric optimization of railway wheel web shape based on fatigue design criteria. Int J Fatigue 134:105463
21. Xiu R, Spiryagin M, Wu Q et al (2021) Fatigue life prediction for locomotive bogie frames using virtual prototype technique. Proc Inst Mech Eng Part F J Rail Rapid Transit 235(9):1122–1131
22. European Committee for Standardization (2023) Railway applications – Wheelsets and bogies – Method of specifying the structural requirements of bogie frames (EN 13749:2021+A1:2023)
23. Cascino A, Meli E, Rindi A (2024) Development of a design procedure combining topological optimization and a multibody environment: application to a tram motor bogie frame. Vehicles 6(4):1843–1856
24. Mi C, Li W, Xiao X et al (2019) Lifetime assessment and optimization of a welded A-type frame in a mining truck considering uncertainties of material properties and structural geometry and load. Appl Sci 9(5):918
25. Zhou W, Zhang G, Wang H et al (2022) Experimental fatigue evaluation of bogie frames on metro trains. Machines 10(11):1003
26. Guo F, Wu SC, Liu JX et al (2020) Fatigue life assessment of bogie frames in high-speed railway vehicles considering gear meshing. Int J Fatigue 132:105353
27. Jameson A (1995) Gradient based optimization methods. MAE Technical Report No.2057, Princeton University
28. Ministero delle Infrastrutture e dei Trasporti, Direzione Generale per le Investigazioni Ferroviarie (2012) Relazione di indagine sull'incidente ferroviario del 29 giugno 2009 nella stazione di Viareggio (Investigation report on the railway accident of 29 June 2009 at Viareggio station). https://www.studio-gabrielli.it/documenti/relazione-viareggio-2009.pdf. Accessed 10 January 2025
29. European Committee for Standardization (2011) Railway applications – Requirements for bogies and running gears (EN 15827:2011). CEN, Brussels
30. European Committee for Standardization (2023) Railway applications – Welding of railway vehicles and components – Part 3: Design requirements (EN 15085–3:2023). CEN, Brussels
31. European Committee for Standardization (2006) Hot finished structural hollow sections of non-alloy and fine grain steels – Part 1: Technical delivery conditions (EN 10210–1:2006). CEN, Brussels
32. European Committee for Standardization (2004) Hot rolled products of structural steels – Part 2: Technical delivery conditions for non-alloy structural steels (EN 10025–2:2004). CEN, Brussels
33. European Committee for Standardization (2006) Steels for quenching and tempering – Part 1: General technical delivery conditions (EN 10083–1:2006). CEN, Brussels
34. European Committee for Standardization (2024) Railway applications – Strength assessment of rail vehicle structures – Part 1: General (EN 17149–1:2024). CEN, Brussels
35. European Rail Research Institute (1997) Programme of tests to be carried out on wagons with steel underframe and body structure (suitable for being fitted with the automatic buffing and draw coupler) and on their cast steel frame bogies (ERRI B 12/RP 17). ORE, Utrecht
36. European Rail Research Institute (1998) Limit stress evaluation and fatigue assessment for bogies and vehicle bodies (ERRI B 12/RP 60). ORE, Utrecht
37. Yüksel Ç (2020) Microstructural analysis of EN-GJS-450-10 ductile cast iron via vibrational casting. China Foundry 17(4):272–278
38. Cascino A, Meli E, Rindi A (2024) A new strategy for railway bogie frame designing combining structural–topological optimization and sensitivity analysis. Vehicles 6(2):651–665